

Reactions of PO_xCl_y^- Ions with H and H_2 from 298 to 500 K

Anthony J. Midey,* Thomas M. Miller, Robert A. Morris, and A. A. Viggiano

Air Force Research Laboratory, Space Vehicles Directorate, 29 Randolph Road,
Hanscom AFB, Massachusetts 01731-3010

Received: October 20, 2004; In Final Form: December 23, 2004

Rate constants and product branching ratios for PO_xCl_y^- ions reacting with H and H_2 were measured in a selected ion flow tube (SIFT) from 298 to 500 K. PO_2Cl^- , PO_2Cl_2^- , POCl_2^- , and POCl_3^- were all unreactive with H_2 , having a rate constant with an upper limit of $<5 \times 10^{-12} \text{ cm}^3 \text{ s}^{-1}$. PO_2Cl_2^- did not react with H atoms either, having a similar rate constant limit of $<5 \times 10^{-12} \text{ cm}^3 \text{ s}^{-1}$. The rate constants for PO_2Cl^- , POCl_2^- , and POCl_3^- reacting with H showed no temperature dependence over the limited range of 298–500 K and were approximately 10–20% of the collision rate constant. Cl abstraction by H to form HCl was the predominant product channel for PO_2Cl^- , POCl_2^- , and POCl_3^- , with a small amount of Cl^- observed from $\text{POCl}_2^- + \text{H}$. Reactions of O_2 and O_3 with the POCl^- products ions from the reaction of $\text{POCl}_2^- + \text{H}$ were observed to yield predominantly PO_3^- and PO_2^- , respectively. POCl^- reacted with O_2 and O_3 with rate constants of $8.9 \pm 1.1 \times 10^{-11}$ and $5.2 \pm 3.3 \times 10^{-10} \text{ cm}^3 \text{ s}^{-1}$, respectively. No associative electron detachment in the reactions with H atoms was observed with any of the reactant ions; however, detachment was observed with a PO^- secondary product ion at high H atom concentrations. Results of new G3 theoretical calculations of optimized geometries and energies for the products observed are discussed.

Introduction

Recently, reactions of various positive and negative ions with H and H_2 have been studied to ascertain their relevance to the space environment.^{1–4} H_2 and H are important species in combustion processes as well. Ion–molecule chemistry from air plasmas has been shown to be a viable method for enhancing combustion.^{5,6} However, the role of negative ion chemistry in combustion is not as well understood. In addition, oxyphosphorus compounds have been shown to be reasonable alternatives to phosphine additives for hydrogen-fueled scramjet combustors, yielding a measurable increase of the flameholding stability and output thrust in the supersonic expansion because of enhanced H, O, and OH recombination kinetics.⁷ Flames doped with oxyphosphorus compounds have also been observed to produce anions of these compounds whose profile along the flame axis is strongly influenced by reactions with H as well as H_2 .⁸

The chemistry of anions generated from phosphorus oxychloride, POCl_3 , has recently been studied in our laboratory using a selected ion flow tube (SIFT).⁹ POCl_3 is known to generate Cl^- , POCl_2^- , and POCl_3^- by dissociative electron attachment.^{10,11} Therefore, the rate constants and product branching ratios of PO_xCl_y^- ion reactions with H_2 and H, including PO_2Cl_2^- and PO_2Cl^- ions produced by source chemistry from POCl_3 ,¹² have been measured in the SIFT from 298 to 500 K. The current experiments address the issues outlined above and further our recent studies of O_2 and O_3 reactions with these ions.⁹

Experimental Section

(a) Kinetics Measurements. The SIFT instrument at the Air Force Research Laboratory has been described in detail elsewhere¹³ and will only briefly be described with regard to the current experiments. All of the reagents have been used as obtained from the manufacturer except for POCl_3 , which was

subjected to several freeze–pump–thaw cycles to remove dissolved gases. Electron impact on POCl_3 (Aldrich, 99%) in an effusive source using a thoriated iridium filament produced ions which were mass selected by a quadrupole mass filter and injected into a fast flow of helium buffer gas (AGA, 99.997%). The buffer gas was introduced into the flow tube through a Venturi inlet and entrained the injected ions. The He used for the buffer flow and discharge source was passed through a liquid-nitrogen-cooled sieve trap to remove water vapor and other trace impurities before entering both the flow tube and atom source. H atoms were generated by a microwave discharge on a mixture of He and H_2 (Matheson, 99.9999%) in a Pyrex tube. Typical H_2 dissociation fractions were 5–10%. The reaction with H_2 alone was studied first because H and H_2 were added simultaneously to the reaction region. The remaining parent ions and any product ions were sampled through a blunt nose cone aperture and mass analyzed with a second quadrupole mass filter and detected.

Product branching ratios were obtained by extrapolating the measured branching ratios to zero neutral concentration to minimize the effects of secondary chemistry. The product branching ratios for the major species have uncertainties of $\pm 10\%$.¹⁴ The H atom concentration was calibrated by the known rate constant for Cl^- reacting with H of $9.6 \times 10^{-10} \text{ cm}^3 \text{ s}^{-1}$, which does not vary over our temperature range.^{15,16} The rate constants for the H atom reactions have relative uncertainties of $\pm 20\%$ and absolute uncertainties of $\pm 30\%$, slightly higher than for stable gases such as H_2 , which have relative and absolute uncertainties of $\pm 15\%$ and $\pm 25\%$, respectively.¹³ In addition, the ion current at the nose cone can be monitored as a function of both the H atom concentration and total ion counts to determine if associative detachment occurred, because product electrons diffuse rapidly to the walls resulting in a decrease in nose cone current.^{17,18}

To probe for reaction pathways to PO_3^- and PO_2^- ions previously observed in POCl_3 doped flames,¹⁹ the chemistry of

* Corresponding author. E-mail: anthony.midey@hanscom.af.mil.

TABLE 1: Rate Constants and Branching Ratios for the Reaction of $\text{PO}_x\text{Cl}_y^- + \text{H}$ and Secondary Product Ion Chemistry^a

reactants	products	$\Delta H_{298\text{K}}^0$ kJ mol ⁻¹	rate constant, [k_c] ($\times 10^{-9}$ cm ³ s ⁻¹) branching ratios	
			300 K	500 K
$\text{PO}_2\text{Cl}^- + \text{H} \rightarrow$	$\text{PO}_2^- + \text{HCl}$	-222	0.36 [1.9]	0.37 [1.9]
	$\text{HOPOCl} + \text{e}^-$	7	1.00	1.00
$\text{PO}_2\text{C}_2^- + \text{H} \rightarrow$	$\text{PO}_2\text{Cl}^- + \text{HCl}$	-27	<0.005 [1.9] No Rxn.	<0.005 [1.9] No Rxn.
$\text{POCl}_2^- + \text{H} \rightarrow$	$\text{POCl}^- + \text{HCl}$	-45	0.16 [1.9]	0.16 [1.9]
	$\text{Cl}^- + \text{HPOCl}$	-6	0.94	0.96
	$\text{HOPCl}_2 + \text{e}^-$	-10	0.06	0.04
	$\text{O}=\text{PHCl}_2 + \text{e}^-$	-3		
$\text{POCl}_3^- + \text{H} \rightarrow$	$\text{POCl}_2^- + \text{HCl}$	-275	0.38 [1.9]	0.37 [1.9]
	$\text{HOPCl}_3 + \text{e}^-$	44	1.00	1.00
secondary	chemistry			
$\text{POCl}^- + \text{O}_2 \rightarrow$	$\text{PO}_3^- + \text{Cl}$	-4.08	0.089 [0.62] >0.99	
	$\text{PO}_2^- + \text{ClO}$	-116	<0.01	
$\text{POCl}^- + \text{O}_3 \rightarrow$	$\text{PO}_2^- + \text{ClO}_2$	-45	0.52 [0.92] ~0.80	
	$\text{PO}_2^- + \text{Cl} + \text{O}_2$	-32		
	$\text{PO}_2\text{Cl}^- + \text{O}_2$	-240	~0.20	

^a The measured rate constant is given with the Su-Chesnavich collision rate constant value in brackets,^{28,29} both in units of 10^{-9} cm³ s⁻¹. The heat of reaction at 298 K, $\Delta H_{298\text{K}}^0$, has been calculated with G3 theory using the values of Fernandez et al.⁹ and those given in Table 2. All of the ions below are unreactive with H₂, having an upper limit to the rate constant of $<5 \times 10^{-12}$ cm³ s⁻¹. See text for details.

POCl^- ions that were observed as product ions in the current H atom experiments has been studied as follows. H atoms were added at an upstream inlet to produce POCl^- from $\text{POCl}_2^- + \text{H}$. First, O₂ separately and then a 3% O₃ in O₂ mixture²⁰ were introduced at a downstream inlet to react with the POCl^- ions, and the rate constants and relative branching ratios were measured for O₂ and then O₃. It is optimal if a sufficient amount of H atoms can be added to drive the $\text{POCl}_2^- + \text{H}$ reaction to

completion before examining the secondary chemistry of the products. However, the reaction conditions could not be adjusted to achieve this condition given the H atom concentrations achievable with the current source. Consequently, a large POCl_2^- signal remained along with a large Cl^- signal arising from the $\text{POCl}_2^- + \text{O}_3$ reaction, where Cl^- accounted for >75% of the reactivity.⁹ The POCl^- signal was much smaller than both the remaining POCl_2^- and the Cl^- signal just described, meaning that any increase in Cl^- would have been a small addition to a large peak that could not be measured. It should also be noted that the operating conditions of the mass spectrometer needed to resolve $m/z = 79$ (PO_3^-) vs $m/z = 82$ (POCl^-) severely discriminated against $m/z = 35$. Thus, these conditions precluded determining the branching ratio of Cl^- that might be generated by the POCl^- reaction. Nevertheless, the mass discrimination against $m/z = 63$ (PO_2^-) is much less severe, and a correction to the branching ratios for the O₂ and O₃ reactions was subsequently applied. Thus, the branching ratios for this secondary chemistry with O₂ and O₃ neglect any contribution from Cl^- products from these reactions. All of the experimental results are given in Table 1.

(b) Structure Calculations. The total energy at 0 K and the enthalpy at 298 K for optimized geometries of the relevant molecular species have been calculated with G3 theory^{21,22} using Gaussian 03W²³ with the results shown in Table 2. The structural parameters given in Tables 3 and 4 were determined from the MP2(Full)/6-31G(d) optimization step of G3. Electron affinities (EA) were also determined for PO, PO_2Cl , and POCl and are compared with literature values.^{9,10,24–26}

The wave function stability of the molecules shown in Tables 2–4 was verified for the Hartree–Fock (HF) level optimization step of G3. However, two exceptions required additional calculations to obtain geometries with a corresponding stable wave function. A stable wave function at the HF level could not easily be obtained for the isomers P–O–H and O=PHOCl, molecules that could be produced via associative detachment of H to PO^- and PO_2Cl^- , respectively. Consequently, G3(B3LYP) calculations²⁷ were performed for two sets of related species: the POH and HPO isomers and the HPO_2Cl , O=PHOCl, PO_2Cl , PO_2Cl^- , and H reactants and products. Performing the additional calculations at the same level for all of the related molecules allowed for comparisons of the relative energies and enthalpies

TABLE 2: G3 Total Energies, Enthalpies, and Electron Affinities (EA)^g

	total energy (0 K)	enthalpy (298 K)	EA (calc.)	EA (lit.)
PO ($C_{\infty v}$, ² Π_g)	-416.372258	-416.368940	1.103	1.092, ^a 1.00 ^b
PO^- ($C_{\infty v}$, ³ Σ^-)	-416.412774	-416.409438		
O=POO (C_s , ² A'')	-566.653441	-566.648080	3.311	
O=POO ⁻ (C_s , ¹ A')	-566.775100	-566.769614		
POCl (C_s , ¹ A')	-876.499870	-876.495344	1.342	1.06, ^c 1.25 ^d
POCl^- (C_s , ² A'')	-876.549106	-876.544227		
PO_2Cl (C_{2v} , ¹ A_1)	-951.716178 ^e	-951.711027 ^e	2.109 ^e	2.145 ^f
PO_2Cl^- (C_s , ² A')	-951.793661 ^e	-951.788053 ^e		
HP=O (C_s , ¹ A')	-416.976138	-416.972310		
HO–PCL (C_1 , ² A)	-877.064143	-877.059023		
O=PH–Cl (C_1 , ² A)	-877.050838	-877.046188		
HO–PCL ₂ (C_s , ¹ A')	-1337.185569	-1337.179430		
O=PH–Cl ₂ (C_s , ¹ A')	-1337.182583	-1337.176990		
HOPCl ₃ (C_1 , ² A)	-1797.214934	-1797.206856		
HO–POCl (C_1 , ² A)	-952.283854	-952.278005		
	-952.288108 ^e	-952.282096 ^e		
O=PHOCl (C_s , ² A'')	-952.243667 ^e	-952.238088 ^e		
H (² $S_{1/2}$)	-0.501003	-0.498632		
	-0.501087 ^e	-0.498726 ^e		
HCl ($C_{\infty v}$, ¹ Σ^+)	-460.654664	-460.651360		

^a Zittel and Linerberger.²⁴ ^b Wu and Tiernan.²⁵ ^c Miller et al., MP4 theory.¹⁰ ^d Miller et al., G2 theory.²⁶ ^e Calculated using G3(B3LYP) method. See text for details. ^f Fernandez et al., G3 theory.⁹ ^g All units except EA are in hartrees. EA values are in eV.

TABLE 3: Bond Lengths (Å) and Angles (degrees) for Geometries from G3 Theory

parameter	O=P=Cl	O=P=Cl ⁻	HOPCl	O=PHCl	HP=O
$r(\text{P}-\text{O})$	1.493	1.533	1.647	1.488	1.517
$r(\text{P}-\text{Cl})$	2.078	2.390	2.072	2.038	
$r(\text{P}-\text{H})$				1.418	1.453
$r(\text{O}-\text{H})$			0.976		
$\angle(\text{Cl}-\text{P}-\text{O})$	110.5	110.6	102.1	118.9	
$\angle(\text{H}-\text{P}-\text{O})$				116.7	105.6
$\angle(\text{H}-\text{P}-\text{Cl})$				99.4	
$\angle(\text{P}-\text{O}-\text{H})$			114.7		
dihedral $\angle(\text{Cl}-\text{P}-\text{O}-\text{H})$			46.2		

parameter	HOPCl ₃	HOPCl ₂	O=PHCl ₂	HOP=OCl
$r(\text{P}-\text{O}^1)$	1.618	1.628	1.480	1.489 ^a
$r(\text{P}-\text{O}^2)$				1.629
$r(\text{P}-\text{Cl}^1)$	2.194	2.073	2.016	2.041
$r(\text{P}-\text{Cl}^2)$	2.098	2.073	2.016	
$r(\text{P}-\text{Cl}^3)$	2.033			
$r(\text{P}-\text{H})$			1.399	
$r(\text{O}-\text{H})$	0.979	0.979		0.979
$\angle(\text{Cl}^1-\text{P}-\text{O}^1)$	95.6	101.4	115.7	117.7
$\angle(\text{Cl}^1-\text{P}-\text{O}^2)$				100.3
$\angle(\text{Cl}^2-\text{P}-\text{O}^1)$	94.1	101.4	115.7	
$\angle(\text{Cl}^3-\text{P}-\text{O}^1)$	105.3			
$\angle(\text{Cl}^1-\text{P}-\text{Cl}^2)$	147.6	99.2	103.2	
$\angle(\text{Cl}^1-\text{P}-\text{Cl}^3)$	102.9			
$\angle(\text{Cl}^2-\text{P}-\text{Cl}^3)$	104.2			
$\angle(\text{H}-\text{P}-\text{O}^1)$			117.1	
$\angle(\text{H}-\text{P}-\text{O}^2)$			101.4	
$\angle(\text{H}-\text{P}-\text{Cl}^2)$			101.4	
$\angle(\text{P}-\text{O}-\text{H})$	111.5	115.9		109.9
$\angle(\text{O}-\text{P}-\text{O})$				116.0
dihedral	-19.3	-51.0		-143.8
$\angle(\text{Cl}^1-\text{P}-\text{O}-\text{H})$				
dihedral	-168.3	51.0		
$\angle(\text{Cl}^2-\text{P}-\text{O}-\text{H})$				
dihedral	85.7			
$\angle(\text{Cl}^3-\text{P}-\text{O}-\text{H})$				
dihedral				-15.9
$\angle(\text{O}^1-\text{P}-\text{O}^2-\text{H})$				

^a P-O¹ is a double bond, P-O² is a single bond.

TABLE 4: Bond Lengths (Å) and Angles (degrees) for Geometries from G3 Theory

parameter	P=O	P=O ⁻	O=POO	O=POO ⁻
$r(\text{P}-\text{O}^1)$	1.538	1.595	1.487 ^a	1.519 ^a
$r(\text{P}-\text{O}^2)$			1.704	1.601
$r(\text{O}^2-\text{O}^3)$			1.372	1.514
$\angle(\text{O}^1-\text{P}-\text{O}^2)$			105.2	110.8
$\angle(\text{P}-\text{O}^2-\text{O}^3)$			115.7	98.7
dihedral $\angle(\text{O}-\text{P}-\text{O}-\text{O})$			180.0	180.0

^a P-O¹ is the terminal P-O double bond.

of reaction and for determination of stable wave functions, where the geometries were optimized using density functional theory (DFT) at the B3LYP/6-31G(d) level for G3(B3LYP).

The wave functions of these oxyphosphorus compounds using G3(B3LYP) were all stable using DFT, with the only exception still being the high-lying P-O-H isomer. However, this isomer lies ca. 1.5 eV higher in energy than H-P=O according to both the G3 and DFT calculations. Although the energy of the optimized wave function is thus somewhat uncertain, the P-O-H isomer would still be inaccessible at the temperatures studied here. The G3(B3LYP) energies are also given in Table 2.

Results and Discussion

(a) H and H₂ Reactions. Rate constants and branching ratios for the reactions of PO_2Cl^- , PO_2Cl_2^- , POCl_2^- , and POCl_3^- with

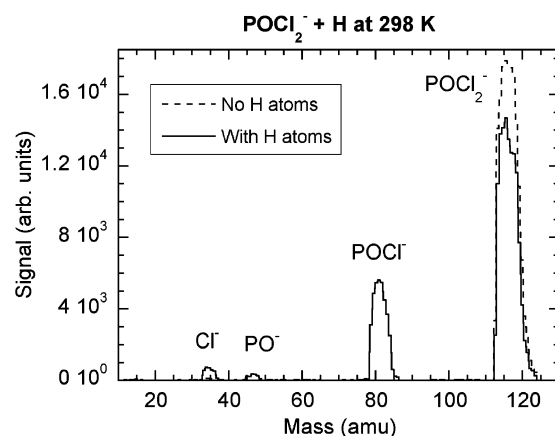
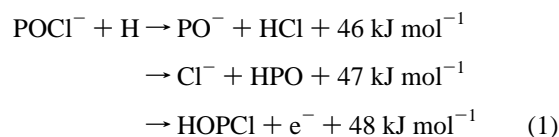


Figure 1. Mass spectra for the reaction of POCl_2^- with H at 298 K as measured in the selected ion flow tube (SIFT). The dashed line is without any H atoms in the flow tube and the solid line is with H atoms added to the flow tube.

H and H₂ measured from 298 to 500 K are shown in Table 1. The enthalpies of reaction at 298 K, $\Delta H_{298\text{K}}^0$, are included in Table 1 and have been determined from both the previous⁹ and new G3 calculations. The new G3 calculations of the total energy at 0 K and the enthalpy at 298 K are presented in Table 2, representing optimized structures given in Tables 3 and 4 as mentioned above. None of the ions currently studied react with H₂ to a measurable extent; therefore, the limitations of the instrument permit only an upper bound for the rate constant of $<5 \times 10^{-12} \text{ cm}^3 \text{ s}^{-1}$ for the H₂ reaction. PO_2Cl_2^- is unreactive with H atoms as well. A comparable limit can be placed on the rate constant for this reaction since no products were observed. A similar lack of reactivity of PO_2Cl_2^- with O₂, O₃, and even POCl_3 has been previously observed in the SIFT.^{9,12} This ion is very stable as evidenced by G3 calculations (EA $\text{PO}_2\text{Cl}_2 = 5.788 \text{ eV}$)⁹ and is a prominent terminal ionic species in the reaction of POCl_2^- and POCl_3^- with O₃.⁹ The rate constants for the reactive species are roughly 10–20% of the Su-Chesnavichvich collision rate constant^{28,29} and show no temperature dependence over the temperature range of 298–500 K presently studied.

By far the most prevalent channel for all three reactive ions, PO_2Cl^- , POCl_3^- , and POCl_2^- , is Cl abstraction by H to form HCl. Cl abstraction is also exothermic for the PO_2Cl_2^- reaction with H even though the ion proves to be unreactive. Figure 1 shows mass spectra for the POCl_2^- reaction taken with and without H atoms added. The mass spectrum shows almost exclusively POCl_2^- before the H atoms are added. At high concentrations of H atoms, three products are observed: Cl^- , POCl^- , and PO^- . However, PO^- is exclusively a secondary product formed from POCl^- reacting with H as shown in eq 1.



It is not possible to completely deconvolute the secondary chemistry because the reaction of POCl^- with H appears to be near collisional; that is, the secondary chemistry is much faster than the primary chemistry. It is clear, however, that PO^- is formed in that reaction, whereas Cl^- and e^- may also be formed as well as shown in eq 1. The reaction of POCl_2^- with H also has a minor primary product channel giving Cl^- and HPOCl that is only slightly exothermic, but it is possible that the Cl^- product signal is primarily from the POCl^- reaction in eq 1. In

addition, PO^- has been observed to undergo associative detachment with H, making it hard to distinguish if POCl^- does as well. Nevertheless, forming POHCl with the H bound to the O via this route is 48 kJ mol^{-1} (0.50 eV) exothermic based on the current G3 theoretical results in Table 2.

An interesting observation is that none of the primary PO_3Cl_y^- ions studied undergo associative detachment with H atoms. The reaction of POCl_2^- with H is $\geq 3 \text{ kJ mol}^{-1}$ (0.03 eV) exothermic for either HPOCl_2 isomer as shown in Table 1, perhaps indicating barriers to forming the neutral product. Previous studies of PO^- ion reactions have found that PO^- was very difficult to make in the ion source of the SIFT so that insufficient signal was available for measuring the rate constant for the H atom reaction, given the relatively low total concentrations of H as well.³⁰ The final product fractions in Table 1 have been corrected for the secondary chemistry of the product ions.

As mentioned above, the G3 results in Tables 2–4 show that a stable minimum energy structure for POHCl exists having an H bound to the O atom with the O–H bond slightly displaced from the Cl–P–O plane. Another stable structure of HPOCl with H bound to the P atom lies 0.36 eV higher in energy. All of the other neutral molecules containing H shown in Tables 2 and 3 also have the lowest energy structure with H bound to O (using G3 theory). The only exception is H–P=O , which is ca. 1.5 eV more stable than P–O–H as discussed above. For HPO_2Cl , the isomer having a P–H bond is 1.21 eV higher in energy using G3(B3LYP). Therefore, this isomer will not play a role up to 500 K. Interestingly, the O–H bond that forms is $\sim 0.98 \text{ \AA}$ in all of the optimized structures shown.

The bond lengths and angles for the POCl neutral calculated here agree well with previous experimental³¹ and theoretical^{31–33} values. The EA for POCl of 1.34 eV calculated here agrees better with the G2 value of Miller et al.²⁶ of 1.26 eV than with the lower level MP2 value of 1.06 eV.¹⁰ The G3 EA of PO of 1.10 eV is in good agreement with the experimental value of Zittel and Lineberger of 1.092 eV from photoelectron spectroscopy,²⁴ values which are both higher than the 1.00 eV value of Wu and Tiernan.²⁵ G3(B3LYP) calculations for PO_2Cl and PO_2Cl^- give an EA of 2.109 eV, in excellent agreement with the G3 value calculated recently.⁹ The present bond lengths for PO and PO^- are both ca. 0.06 \AA longer than the literature values.³⁴ The molecular parameters for HPO are in good agreement with experimental³⁵ and higher level theoretical values,^{35,36} with the current MP2 P–O bond length being ca. 0.03 \AA longer than these values.^{35,36}

(b) Pathways to PO_2^- and PO_3^- . The flame results of Goodings and co-workers show that PO_3^- and PO_2^- are the main ions observed when POCl_3 is added to an atmospheric pressure methane–oxygen flame.¹⁹ One potential first step in the process is electron attachment to form POCl_3^- and POCl_2^- . Since the flame is at atmospheric pressure, the former may dominate.¹¹ Our combined work on the H, O_2 and O_3 reactions shows that only a minor route exists for generating PO_3^- from the reactions of POCl_2^- and POCl_3^- , both of which can be produced by electron attachment to POCl_3 as just discussed.^{10,11} For example, POCl_3^- reacts with H to form POCl_2^- which is also formed directly in electron attachment. However, there is only a minor channel in the reaction of POCl_2^- with ozone that forms PO_3^- (ca. 1%).

As seen in Table 1, POCl^- reacts with O_2 with a rate constant of $8.9 \pm 1.1 \times 10^{-11} \text{ cm}^3 \text{ s}^{-1}$ to form $>99\%$ PO_3^- at 298 K, with a trace amount of PO_2^- also observed. Correcting the O_3 branching ratios and rate constants for the O_2 reaction is also required, and the results for O_3 in Table 1 reflect these

corrections. After making this correction, as well as correcting for the $\sim 1\%$ PO_3^- contribution from the POCl_2^- reaction with O_3 , the branching ratios for POCl^- reacting with O_3 are ca. 0.80 PO_2^- and 0.20 PO_3^- at 298 K. The rate constant for the $\text{POCl}^- + \text{O}_3$ reaction is $5.2 \pm 3.3 \times 10^{-10} \text{ cm}^3 \text{ s}^{-1}$. This measurement has a much larger error limit than typical measurements because of the small concentration of O_3 and the small deviations in successive rate constant measurements that accumulate when correcting for the O_2 reactivity. Nevertheless, these results clearly show that the reaction of POCl_2^- with H is the first step in a pathway to both PO_2^- and PO_3^- .

The minimum energy structures for PO_3 and PO_3^- have been shown to be planar with three equal P–O double bonds in the anion.⁹ New G3 calculations show that peroxide forms of PO_3 and PO_3^- exist having stable planar z-shaped structures with the parameters given in Table 4. This neutral PO_3 isomer is 3.199 eV higher in energy than the ground-state PO_3 , whereas the analogous PO_3^- isomer is 5.044 eV higher than the planar ground-state PO_3^- anion. Even though the reaction of POCl^- with O_2 is 408 kJ mol^{-1} (4.23 eV) exothermic, this higher energy form of PO_3^- will not be accessible in the current temperature range. However, this species may become important at higher temperatures.

Conclusions

The rate constants and branching ratios for the reactions of PO_2Cl^- , PO_2Cl_2^- , POCl_2^- , and POCl_3^- with H and H_2 have been measured in the SIFT from 298 to 500 K. None of the ions react with H_2 , and PO_2Cl_2^- does not react with H either, placing a limit on the rate constant of $<5 \times 10^{-12} \text{ cm}^3 \text{ s}^{-1}$ for all of the systems where no reaction was observed. The rate constants for H atom reactions are $<20\%$ of the collision rate constant and do not vary with temperature from 298 to 500 K. The only product observed is Cl abstraction by H, except for a minor reaction pathway with POCl_2^- that produces Cl^- and HOPCl . Combining the present results with the O_3 reactions studied previously⁹ shows that a pathway from electrons to PO_2^- and PO_3^- exists for methane–oxygen flames doped with POCl_3 ,¹⁹ where the H atom reaction products can react with O_2 and O_3 . In the future, we also plan to examine reactions with O atoms and $\text{O}_2(a^1\Delta_g)$ for more robust pathways to PO_3^- and PO_2^- .

Acknowledgment. We thank John Williamson and Paul Mundis for technical support. This work was supported by the Air Force Office of Scientific Research under Program Number EP2303BMA1. A.J.M. and T.M.M. are under contract to Visidyne, Inc. through Contract Number F19628-99-C-0069.

References and Notes

- (1) Scott, G. B. I.; Fairley, D. A.; Freeman, C. G.; McEwan, M. J.; Adams, N. G.; Babcock, L. M. *J. Phys. Chem. A* **1997**, *101*, 4973–4978.
- (2) Scott, G. B. I.; Fairley, D. A.; Freeman, C. G.; McEwan, M. J.; Spanel, P.; Smith, D. *J. Chem. Phys.* **1997**, *106*, 3982–3987.
- (3) McEwan, M. J.; Scott, G. B. I.; Adams, N. G.; Babcock, L. M.; Terzieva, R.; Herbst, E. *Astrophys. J.* **1999**, *513*, 287–293.
- (4) Barckholtz, C.; Snow, T. P.; Bierbaum, V. M. *Astrophys. J.* **2001**, *547*, L171–L174.
- (5) Williams, S.; Midey, A. J.; Arnold, S. T.; Bench, P. M.; Viggiano, A. A.; Morris, R. A.; Maurice, L. Q.; Carter, C. D. "Progress on the Investigation of the Effects of Ionization on Hydrocarbon/Air Combustion Chemistry"; AIAA 99-4907, 9th International Space Planes and Hypersonic Systems and Technologies Conference, 1999, Norfolk, VA.
- (6) Williams, S.; Midey, A. J.; Arnold, S. T.; Miller, T. M.; Bench, P. M.; Dressler, R. A.; Chiu, Y.-H.; Levandier, D. J.; Viggiano, A. A.; Morris, R. A.; Berman, M. R.; Maurice, L. Q.; Carter, C. D. "Progress on the investigation of the effects of ionization on hydrocarbon/air combustion chemistry: kinetics and thermodynamics of C6–C10 hydrocarbon ions";

AIAA 2001-2873, AIAA 4th Weakly Ionized Gases Workshop, 2001, Anaheim, California.

(7) Pellett, G. L. *NASA Technical Report* **1996**, 1–16.

(8) Goodings, J. M.; Hassanali, C. S. *Int. J. Mass Spectrom. Ion Proc.* **1990**, *101*, 337–354.

(9) Fernandez, A. I.; Midey, A. J.; Miller, T. M.; Viggiano, A. A. *J. Phys. Chem. A* **2004**, *108*, 9120–9125.

(10) Miller, T. M.; Seeley, J. V.; Knighton, W. B.; Meads, R. F.; Viggiano, A. A.; Morris, R. A.; Van Doren, J. M.; Gu, J.; Schaefer, H. F., III *J. Chem. Phys.* **1998**, *109*, 578–584.

(11) Williamson, D. H.; Mayhew, C. A.; Knighton, W. B.; Grimsrud, E. P. *J. Chem. Phys.* **2000**, *113*, 11035–11043.

(12) Morris, R. A.; Viggiano, A. A. *Int. J. Mass Spectrom. Ion Proc.* **1997**, *164*, 35.

(13) Viggiano, A. A.; Morris, R. A.; Dale, F.; Paulson, J. F.; Giles, K.; Smith, D.; Su, T. *J. Chem. Phys.* **1990**, *93*, 1149–1157.

(14) Arnold, S. T.; Williams, S.; Dotan, I.; Midey, A. J.; Morris, R. A.; Viggiano, A. A. *J. Phys. Chem. A* **1999**, *103*, 8421–8432.

(15) Fehsenfeld, F. C. Associative detachment. In *Interaction Between Ions and Molecules*; Ausloos, P., Ed.; Plenum: New York, 1975; Vol. 6, pp 387–412.

(16) Howard, C. J.; Fehsenfeld, F. C.; McFarland, M. *J. Chem. Phys.* **1974**, *60*, 5086.

(17) Ferguson, E. E.; Fehsenfeld, F. C.; Schmeltekopf, A. L. Flowing afterglow measurements of ion–neutral reactions. In *Advances in Atomic and Molecular Physics*; Bates, D. R., Ed.; Academic: New York, 1969; Vol. 5, pp 1–56.

(18) Viggiano, A. A.; Morris, R. A.; Paulson, J. F.; Ferguson, E. E. *J. Phys. Chem.* **1990**, *94*, 7111.

(19) Horton, J. H.; Crovisier, P. N.; Goodings, J. M. *Int. J. Mass Spectrom. Ion Proc.* **1992**, *114*, 99–121.

(20) Williams, S.; Campos, M. F.; Midey, A. J.; Arnold, S. T.; Morris, R. A.; Viggiano, A. A. *J. Phys. Chem. A* **2002**, *106*, 997–1003.

(21) Curtiss, L. A.; Redfern, P. C.; Raghavachari, K.; Pople, J. A. *J. Chem. Phys.* **1998**, *109*, 42.

(22) Curtiss, L. A.; Redfern, P. C.; Raghavachari, K.; Rassolov, V.; Pople, J. A. *J. Chem. Phys.* **1998**, *109*, 7764–7776.

(23) Frisch, M. J.; Trucks, G. W.; Schlegel, H. B.; Scuseria, G. E.; Robb, M. A.; Cheeseman, J. R.; Montgomery, J. A., Jr.; Vreven, T.; Kudin, K.

N.; Burant, J. C.; Millam, J. M.; Iyengar, S. S.; Tomasi, J.; Barone, V.; Mennucci, B.; Cossi, M.; Scalmani, G.; Rega, N.; Petersson, G. A.; Nakatsuji, H.; Hada, M.; Ehara, M.; Toyota, K.; Fukuda, R.; Hasegawa, J.; Ishida, M.; Nakajima, T.; Honda, Y.; Kitao, O.; Nakai, H.; Klene, M.; Li, X.; Knox, J. E.; Hratchian, H. P.; Cross, J. B.; Adamo, C.; Jaramillo, J.; Gomperts, R.; Stratmann, R. E.; Yazyev, O.; Austin, A. J.; Cammi, R.; Pomelli, C.; Ochterski, J. W.; Ayala, P. Y.; Morokuma, K.; Voth, G. A.; Salvador, P.; Dannenberg, J. J.; Zakrzewski, V. G.; Dapprich, S.; Daniels, A. D.; Strain, M. C.; Farkas, O.; Malick, D. K.; Rabuck, A. D.; Raghavachari, K.; Foresman, J. B.; Ortiz, J. V.; Cui, Q.; Baboul, A. G.; Clifford, S.; Cioslowski, J.; Stefanov, B. B.; Liu, G.; Liashenko, A.; Piskorz, P.; Komaromi, I.; Martin, R. L.; Fox, D. J.; Keith, T.; Al-Laham, M. A.; Peng, C. Y.; Nanayakkara, A.; Challacombe, M.; Gill, P. M. W.; Johnson, B.; Chen, W.; Wong, M. W.; Gonzalez, C.; Pople, J. A. *Gaussian 03*, revision B.02; Gaussian, Inc.: Pittsburgh, PA, 2003.

(24) Zittel, P. F.; Lineberger, W. C. *J. Chem. Phys.* **1976**, *65*, 1236.

(25) Wu, R. L. C.; Tiernan, T. O. *Bull. Am. Phys. Soc.* **1982**, *27*, 109.

(26) Miller, T. M.; Viggiano, A. A.; Morris, R. A.; Miller, A. E. S. *J. Chem. Phys.* **1999**, *111*, 3309–3310.

(27) Baboul, A. G.; Curtiss, L. A.; Redfern, P. C.; Raghavachari, K. *J. Chem. Phys.* **1999**, *110*, 7650–7657.

(28) Su, T.; Chesnavich, W. J. *J. Chem. Phys.* **1982**, *76*, 5183–5185.

(29) Su, T. *J. Chem. Phys.* **1988**, *89*, 5355.

(30) Morris, R. A.; Viggiano, A. A. *J. Chem. Phys.* **1998**, *109*, 4126.

(31) Brupbacher-Gatehouse, B.; Brupbacher, T. *J. Chem. Phys.* **1999**, *111*, 6300–6310.

(32) Binnewies, M.; Schnockel, H. *Chem. Rev.* **1990**, *90*, 321–330.

(33) Bell, I. S.; Hamilton, P. A.; Davies, P. B. *J. Phys. Chem. A* **1998**, *102*, 8836.

(34) *NIST Chemistry WebBook, NIST Standard Reference Database No. 69*; Linstrom, P. J., Mallard, W. G., Eds.; National Institutes of Standards and Technology: Gaithersburg, MD, 2003; <http://webbook.nist.gov/chemistry>.

(35) Tackett, B. S.; Clouthier, D. J. *J. Chem. Phys.* **2002**, *117*, 10604–10612.

(36) Luna, A.; Merchan, M.; Roos, B. O. *Chem. Phys.* **1995**, *196*, 437.